Earth Surface Processes and Landforms
Earth Surf. Process. Landforms **24,** 503–516 (1999)

SEDIMENT TRANSPORT CAPACITY AND EROSION PROCESSES: MODEL CONCEPTS AND REALITY

C. HUANG*, L. K. WELLS, AND L. D. NORTON

USDA-ARS National Soil Erosion Research Laboratory, 1196 SOIL Bldg, Purdue University, West Lafayette, IN 47907-1196, USA

Received 24 April 1998; Revised 8 October 1998; Accepted 19 October 1998

ABSTRACT

Sediment transport capacity, T_c, defined as the maximum amount of sediment that a flow can carry, is the basic concept in determining detachment and deposition processes in current process-based erosion models. Although defined conceptually and used extensively in modelling erosion, T_c was rarely measured. Recently, a series of laboratory studies designed to quantify effects of surface hydrologic conditions on erosion processes produced data sets feasible to evaluate the concept of T_c. A dual-box system, consisting of a 1·8 m long sediment feeder box and a 5 m long test box, was used. Depending on the relative magnitudes of sediment delivery from feeder and test boxes, five scenarios are proposed ranging from deposition-dominated to transport-dominated sediment regimes. Results showed that at 5 per cent slope under seepage or 10 per cent slope under drainage conditions, the runoff from the feeder box caused additional sediment transport in the test box, indicating a transport-dominated sediment regime. At 5 per cent slope under drainage conditions, deposition occurred at low rainfall intensities. Increases in slope steepness, rainfall intensity and soil erodibility shifted the dominant erosion process from deposition to transport. Erosion process concepts from the Meyer–Wischmeier, Foster–Meyer and Rose models were compared with the experimental data, and the Rose model was found to best describe processes occurring during rain. A process-based erosion model needs to have components that can represent surface conditions and physical processes and their dynamic interactions.

KEY WORDS: soil erosion; sediment transport; erosion model

INTRODUCTION

During rainfall, many physical processes occur simultaneously at the soil surface. Building a conceptual framework for understanding erosion processes started more than 50 years ago when Ellison (1944, 1947a, b, c) and his co-worker (Ellison and Ellison, 1947a, b) proposed to divide erosion processes into four sub-processes: detachment by raindrop impact (D_R), transport by rainsplash (T_R), detachment by surface flow (D_F) and transport by surface flow (T_F). Meyer and Wischmeier (1969), based on Ellison's model, proposed the 'rate-limiting concept' that sediment delivery, q_s, was limited by either the detachment rate ($D_R + D_F$) or the transport capacity ($T_R + T_F$) depending on which had a lower value. Although Meyer and Wischmeier (1969) used different equations for each of the individual processes, the detachment and transport processes are quantified without an explicit coupling between them. This model is called the Meyer–Wischmeier model here.

Foster and Meyer (1972, 1975) proposed a first-order detachment and transport coupling model for rill flow (hereafter called the Foster–Meyer model). This model relates the detachment or deposition rate, D, to the difference between transport capacity, T_c, and sediment load, q_s, or:

$$\mathrm{D} = \alpha\,(T_c - q_s)$$

where α is a rate control constant. When $q_s < T_c$, the flow will cause additional sediment detachment and when $q_s > T_c$, the excessive sediment will deposit. The value T_c, a predefined hypothetical number, becomes the key in determining whether detachment or deposition occurs. The combination of

* Correspondence to: Dr. C. Huang, National Soil Erosion Research Laboratory, 1196 Soil Bldg, Purdue University, West Lafayette, IN 47907-1196, USA. Email: chihua@ecn.purdue.edu

CCC 0197-9337/99/060503–14 $17.50

conceptual frameworks for rainfall-dominated interrill and runoff-dominated rill erosion processes (Meyer *et al.*, 1975) and the Foster–Meyer detachment–transport coupling model for rill erosion led to principal erosion equations in the process-based Water Erosion Prediction Project (WEPP) model (Nearing *et al.*, 1989). In our paper, the Foster–Meyer model is generalized for erosion processes occurring on a plane slope element, an extension beyond the original rill channel definition.

Unlike the Foster–Meyer model which is based on values of q_s and T_c for the net amount of detachment or deposition, Rose *et al.* (1983; also Rose, 1985) proposed a dynamic model which includes three continuous and simultaneous processes: rainfall detachment, runoff detachment and sediment deposition (hereafter the Rose model). In the Rose model, sediment delivery is the balance of these three processes and it does not require a prior calculation of T_c and a coupling relationship to either detachment or deposition process for the final sediment delivery. Another difference between the WEPP and Rose models is the need in the WEPP model to separate into interrill and rill areas for corresponding interrill and rill processes, while such separation is not required in the Rose model (Rose, 1985).

In the past decade, significant efforts have been invested into the development and validation of the WEPP model in the USA. Unfortunately, little work was done to quantify sediment transport capacity and test the validity of the detachment–transport coupling concept. The difficulty of testing these erosion process model concepts is due to the lack of proper experimental procedures and data. Most of these models were defined in a differential sense, in other words, the mass balance equation was written for a unit area on the soil surface. On the other hand, erosion data are mostly collected as sediment delivery at the outlet, representing an integral quantity which has been integrated over space and time. Since it is very difficult to make measurements in a small unit area on the soil surface during the rainfall event in a true differential sense, a less desirable but possible alternative is to measure sediment delivery at different spatial and temporal scales. Under steady-state conditions, this means a data set of sediment delivery from different-sized plots.

Huang *et al.* (1996) conducted a field study on three US midwest soils to evaluate sediment detachment and transport coupling in flow channels. Their data showed that the rill detachment rate was limited to a certain rate despite an increase in the transport capacity of the flow, indicating the lack of a direct coupling between transport and detachment processes. Consequently, Huang *et al.* (1996) concluded that the rate-limiting concept of Meyer–Wischmeier appears to fit the experimental data better than the rate-coupling concept of Foster–Meyer.

Recent laboratory studies further showed that changing the near-surface hydraulic gradient and slope steepness caused changes in both the dominant erosion process and the controlling sediment regime (Huang and Laflen, 1996; Gabbard *et al.*, 1998; Huang, 1998). Under seepage or exfiltration conditions, the surface became more erodible and rilling was the dominant erosion process. The sediment regime became transport limiting. Under drainage (or infiltration) conditions, surface rilling did not occur and sediment delivery was detachment limited. These studies show that rilling can result from a lowering of surface soil strength as the pore water pressure was increased, not just from the flow shear alone.

Since the hydrologic condition can be controlled to create either a detachment-limiting or a transport-limiting sediment regime in the laboratory, it is possible to use this capability in a dual-box arrangement to further study processes of erosion. A dual-box system consists of a sediment source box upslope to a test box. By feeding the sediment from the source box and measuring the sediment output from the test box, we can evaluate the erosion processes occurring in the test box.

Let S(A) be the sediment delivery from the feeder box, S(B) the sediment from the test box without the feeder input and S(C) the sediment delivery from the test box with the feeder input. Depending on magnitudes of S(A), S(B) and S(C), there are five possible scenarios in the test box:

Scenario 1: $S(\mathrm{C}) < S(\mathrm{A})$, net deposition in the test box;
Scenario 2: $S(\mathrm{C}) = S(\mathrm{A})$, simultaneous erosion and deposition, erosion = deposition;
Scenario 3: $S(\mathrm{A}) < S(\mathrm{C}) < S(\mathrm{A}) + S(\mathrm{B})$, simultaneous erosion and deposition, erosion > deposition;

Scenario 4: $S(C) = S(A) + S(B)$, equilibrium, no effects from feeder runoff in the text box;
Scenario 5: $S(C) > S(A) + S(B)$, additional erosion in the test box from the feeder runoff.

Using this dual-box system and prior knowledge of the controlling sediment regime as the hydrologic condition of the test box is changed, we can study conditions when a specific scenario takes place.

The objective of this paper is to identify dominant erosion processes as the surface condition is changed through a series of laboratory rainfall simulations on a dual-box system. Variables changed to create different surface conditions are slope steepness, seepage and drainage, and rainfall intensity. These data sets are used to evaluate the conceptual framework for sediment detachment, deposition and transport processes, especially on the role of sediment transport capacity. Results of this study will further the understanding of erosion processes and provide a framework for developing a process-based erosion model.

A trial run was also conducted to isolate seepage effects on sediment delivery from the increased runoff due to the background seepage flow.

MATERIALS AND METHODS

Soil sample collection and experimental setup

The soil used in this study was an Ava silt loam (fine-silty, mixed, mesic Typic Fragiudalf with 15 per cent sand, 70 per cent silt and 15 per cent clay) collected from Sullivan County, Indiana. The soil was sampled from a grassy area, up to 0·3 m deep, along the shoulder area of a hill. Sufficient soil was transported back to the laboratory for the experiment.

The study was conducted on a dual-box system consisting of a 5 m long test box and a 1·8 m long feeder box (Figure 1). Both boxes are 1·2 m wide and 0.3 m deep. The feeder box sat upslope of the test box. These two boxes can be connected by a connecting piece such that runoff from the feeder box can be fed to the upper end of the test box. When disconnected, runoff samples can be collected separately from each box. The connection and disconnection can be done quickly without stopping the rain.

The slope of the test box was adjustable from 0 to 40 per cent in 5 per cent increments. The test box had 75 watering (or drainage) holes (6 mm diameter) at the bottom. A water circulation system was designed to supply water to the bottom of the test box with a capability of maintaining a constant water level of any position relative to the soil surface. A seepage or exfiltration condition was created when the water level in the water supply tubes was above the soil surface forcing water flow upward through the soil and exfiltrate at the surface. Alternatively, the water supply tubes were lowered below the soil surface to create a tension-assisted drainage condition or disconnected to let the test box drain under gravity. A detailed description of the test box and water circulation system was given by Huang and Laflen (1996) and Gabbard *et al.* (1998).

The feeder box can be set to any slope steepness by hoisting up its upslope end using a pulley-chain system. The feeder box has 27 holes at the bottom (6 mm diameter) for seepage or drainage control. In this study, these holes were open for free drainage.

For both boxes, the depth of soil fill was approximately 25 cm, overlying a 2 cm layer of sand at the bottom. These two boxes were placed under two sets of oscillating-nozzle, programmable rainfall simulation troughs (Foster *et al.*, 1979). There are five rainfall troughs spaced 1 m apart for the test box and three troughs at 0·84 m spacing for the feeder box. Each rain trough had two VeeJet nozzles (Part No. 80100, Spraying Systems Co. Wheaton, IL, USA) spaced 1·07 m apart. Vertical distance between the nozzle and soil surface was approximately 2·8 m for the test box and 2·4 m for the feeder box. During rainfall simulation, the nozzle pressure was kept at 41·4 kPa (6 psi). These two sets of rainfall simulators can be set to selected rainfall intensities, ranging from 25 to 200 mm h^{-1} by programming the oscillating frequency of the nozzles, and controlled independently for different rain intensities on each box.

Preparation of the soil box included adding fresh soil collected from the field, breaking up clods to 2–3 cm in size, and smoothing out the visual irregularities on the surface by hand or a rake. Both boxes

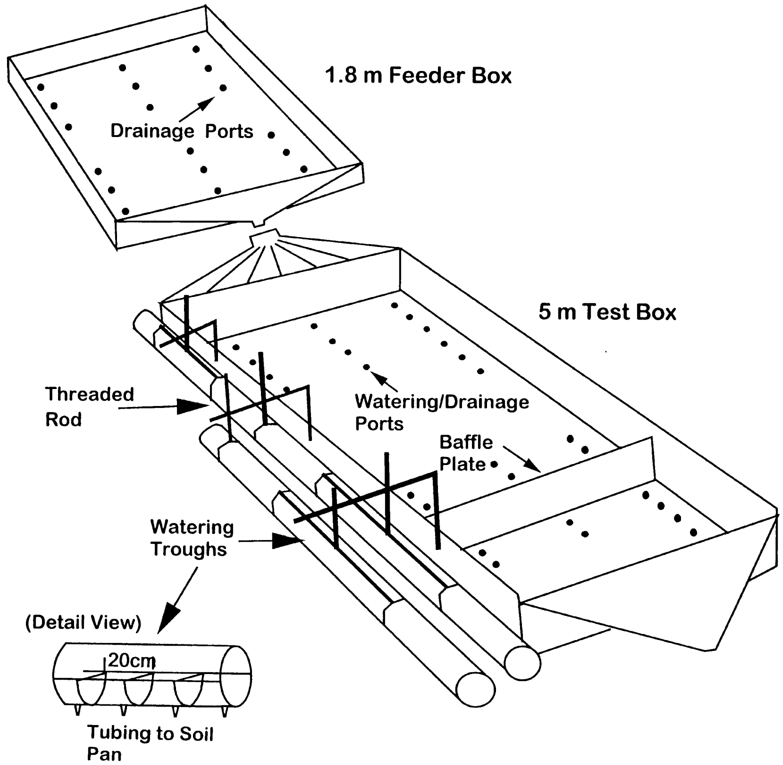

Figure 1. Schematic diagram of the dual-box system

Table I. List of experimental treatments

Treatment no.	Feeder box Slope (%)	Feeder box Rainfall ($mm\,h^{-1}$)	Test box Slope (%)	Test box Hydrology
1	10	100	5	Seepage, +20 cm*
2	10	150	5	Seepage, +20 cm*
3	10	100	5	Drainage, –20 cm*
4	10	150	5	Drainage, –20 cm*
5	10	100	10	Drainage, –20 cm*
6	10	150	10	Drainage, –20 cm*

* Water surface in the watering tube relative to the soil surface

were prepared in the same way. Once the boxes were prepared, they were set to level position and rained on for 30 min at 50 mm h^{-1} intensity. This initial rainstorm, as part of the soil box preparation procedure, was used to wet down the soil surface and to consolidate the loose aggregates to form a wet surface seal. The initial storm also reduced the variability from the surface preparation. After the ponded water from the initial rainstorm had drained from the surface, the test box was set to selected slope steepness and hydrologic (i.e., seepage or drainage) condition (Table I). The feeder box was free drained during the experiment.

Experimental procedure

The erosion study was conducted 24 h after the initial rain. The run consisted of continuous rainfall events of four rainfall intensities (50, 25, 75 and 150 mm h^{-1}) on the test box. The run started with the 50 mm h^{-1} storm on the test box. The rainfall on the feeder box also started at the same time at either 100 or 150 mm h^{-1} for low or high sediment feed rates. Runoff samples from both boxes were collected in 8 l buckets every 3 min. After collecting 10 runoff samples, the two boxes were connected to let the runoff from the feeder box feed to the upper end of the test box. After a waiting period of 1 to 2 min for the surface to 'equilibrate' to the new condition, four runoff samples were collected from the test box which was receiving runoff input from the feeder box. After sampling with the two boxes connected, the connecting piece was removed and two additional runoff samples were collected from each box separately. These two final samples were used to account for the temporal changes of the sediment delivery as the surface is being eroded.

After all the runoff samples were collected for the 50 mm h^{-1} rain, the rain intensity for the test box was switched to 25 mm h^{-1} and the sequence of collecting runoff samples was repeated: from both boxes separately, from test box with runoff input from the feeder box, and again from both boxes separately. The same sampling protocol was repeated for 75 and 150 mm h^{-1} rainstorms on the test box. Instead of taking 10 runoff samples before the feeder box was connected, as was being done during the 50 mm h^{-1}, only four runoff samples were taken for the 25, 75 and 150 mm h^{-1} storms. Throughout the rain sequence, the intensity of the feeder box remained constant, at either 100 or 150 mm h^{-1}. The entire run lasted about 2 h.

After each run, 10 to 20 ml of saturated alum ($AlK(SO_4)_2$) solution was added to the buckets to flocculate the suspended sediment. After settling overnight, the excess water was poured out of the buckets and the sediment was transferred into 1 l bottles. The bottles were placed in ovens at 105°C for at least 24 h or until the sediment samples were dried. Dry weights were then taken to calculate the sediment delivery rate and concentration.

Following the run, the soil boxes were drained and dried under a large fan. After the soil surface was dried, the soil was then turned by a shovel for additional drying of the newly exposed subsurface soil. Fresh, air-dried soil was added to the surface during preparation for the next run. Each run was replicated twice.

The experiments were conducted for combinations of slope steepness, hydraulic gradient, and level of runoff/sediment feed from the feeder box (Table I). These combinations were designed to represent hydrologic conditions that would be expected for a 5 m segment of a hillslope in various topographic positions.

Runs to show seepage effects under similar rainfall and runoff rates

In order to compare the seepage and drainage effects under the same rainfall and runoff intensities, trial runs were made during another study using the same soil. The runs were conducted with the test box first under the seepage condition at 5 per cent slope. After collecting sediment samples, the soil box was drained and additional water was added to the top of the test box to compensate for the runoff difference between background seepage and infiltration. Thus, the subsequent run made under drainage conditions had similar surface morphology, rainfall and runoff intensities to those under seepage condition. Two runs were made, one at 50 mm h^{-1} and the other one at 100 mm h^{-1} rainfall intensity. Two levels of feeder sediment content were also created by covering and uncovering the feeder box surface with a landscape fabric.

Data processing and tabulation

Runoff (R) and sediment (S) rates were averaged from six samples, four before connection and two after disconnection, for both test and feeder boxes and from four samples when two boxes are

Table II. Average runoff (R) and sediment delivery (S) from two trial runs with the test box initially under seepage condition (sp) and subsequently drained and rained again with added inflow (dr) to maintain similar runoff. Two levels of feeder sediment input were created by covering the soil surface with a landscape fabric

Feeder box			Test box		Test box with feeder input	
Cover (%)	R(A) ($l\,h^{-1}$)	S(A) ($kg\,h^{-1}$)	R(B) ($l\,h^{-1}$)	S(B) ($kg\,h^{-1}$)	R(C) ($l\,h^{-1}$)	S(C) ($kg\,h^{-1}$)
Run 1-sp: seepage, rain 50 mm h^{-1}						
0	324	19·2	600	50·0	972	99·8
100	324	1·5	540	34·0	900	66·4
Run 1-dr: drainage, rain 50 mm h^{-1} plus inflow						
100	324	1·4	546	5·8	906	9·0
0	330	22·7	534	6·3	798	15·3
Run 2-sp: seepage, rain 100 mm h^{-1}						
0	324	20·9	936	96·1	1260	136·3
100	318	1·5	876	69·0	1230	96·3
Run 2-dr: drainage, rain 100 mm h^{-1} plus inflow						
100	318	1·6	846	16·5	1152	18·2
0	330	22·8	894	14·0	1230	29·4

connected. These average values are presented in Tables II, III, and IV. In Table IV, sediment scenarios were assigned using an arbitrarily selected threshold value of 2 kg h^{-1}, which means that any two values have to differ by more than the threshold to be considered different. Instead of reporting averages from two runs, individual run data are shown and ranked for the corresponding scenario because each run was a realization of physical processes occurring on the soil surface and averaging may have obscured these individual processes.

RESULTS AND DISCUSSION

Seepage effects on erosion

The surface after the run under seepage conditions at 5 per cent slope showed severe rilling while only crescent-shaped scouring pits were observed under drainage conditions (Figures 2 and 3). Rilling was evident after runs at the 10 per cent slope under drainage conditions. The seepage and slope effects are similar to those observed by Gabbard *et al.* (1998) despite differences in soil and run procedures. Gabbard *et al.* used a clay loam soil, which was much less erodible compared to the silt loam soil used in this study. Gabbard *et al.* (1988) also added inflow water at rates as high as 38 l min^{-1} to plots half as wide (i.e. 0·6 m) while this study used the full box width and the highest discharge was approximately 23 l min^{-1} or 1400 l h^{-1}.

An illustration of seepage effects is depicted in Figure 4 which shows sediment data as a function of runoff from the 5 m test box at 5 per cent slope under different rainfall intensities. The difference in runoff between seepage and drainage conditions under the same rainfall intensity is due to the combination of background seepage flow under seepage conditions and infiltration under drainage conditions. The seepage effect can be examined in three different ways: under the same rainfall and runoff intensities (Table II); under the same rainfall intensity using data tabulated in Table IV; and under the same runoff intensity (Figure 4). Since the background seepage flow carried only negligible amounts of sediment, the additional sediment under seepage conditions resulted from both increased detachment and/or increased flow transport.

Comparison of seepage and drainage effects on sediment delivery can sometimes be difficult owing to greater runoff rates under seepage conditions. The most logical way is to compare runs under similar rainfall and runoff intensities with inflow water added under drainage conditions to raise runoff to levels

Table III. Average run off, R, from individual runs collected from feeder box, R(A), test box alone, R(B) and test box with feeder input R(C)

Run 1					Run 2				
Feeder box	Test box			Test box with feeder input	Feeder box	Test box			Test box with feeder input
R(A) (l h^{-1})	Rain (mm h^{-1})	R(B) (l h^{-1})	R(A) + R(B) (l h^{-1})	R(C) (l h^{-1})	R(A) (l h^{-1})	Rain (mm h^{-1})	R(B) (l h^{-1})	R(A) + R(B) (l h^{-1})	R(C) (l h^{-1})
Treatment 1, Feeder box: rain 100 mm^{-1}; Test box: slope: 5%, + 20 cm seepage									
203	25	365	568	597	193	25	447	641	635
204	50	520	724	735	192	50	577	768	790
203	75	685	888	904	199	75	741	940	935
205	150	1112	1317	1377	203	150	1170	1373	1396
Treatment 2, Feeder box: rain 150 mm^{-1}; Test box: slope: 5%, + 20 cm seepage									
292	25	356	647	621	301	25	356	657	619
296	50	492	788	762	300	50	496	796	799
296	75	642	939	915	299	75	638	937	948
297	150	1080	1377	1369	306	150	1030	1336	1346
Treatment 3, Feeder box: rain 100 mm h^{-1}; Test box: slope: 5%, –20 cm drainage									
192	25	154	347	328	193	25	161	354	351
194	50	256	449	404	189	50	280	469	467
196	75	426	621	614	193	75	433	626	625
197	150	665	862	847	197	150	779	976	978
Treatment 4, Feeder box: rain 150 mm h^{-1}; Test box: slope 5%, –20 cm drainage									
300	25	195	495	481	296	25	182	478	473
306	50	321	627	608	299	50	304	603	597
305	75	471	776	770	297	75	457	754	763
307	150	817	1124	1132	301	150	850	1151	1155
Treatment 5, Feeder box: rain 100 mm h^{-1}; Test box: slope: 10%, –10 cm drainage									
200	25	156	355	352	194	25	156	350	351
201	50	280	480	481	194	50	282	476	475
201	75	423	624	626	194	75	424	618	608
198	150	793	990	950	195	150	752	947	975
Treatment 6, Feeder box: rain 150 mm h^{-1}; Test box: slope: 10%, –10 cm drainage									
290	25	172	462	460	313	25	178	490	490
292	50	292	584	579	306	50	304	610	627
297	75	437	734	731	310	75	449	759	767
301	150	803	1104	1113	313	150	833	1147	1141

Table IV. Average sediment delivery, S, from individual runs collected from feeder box, S(A), test box alone, S(B) and test box with feeder input S(C)

Run 1						Run 2					
Feeder box	Test box			Test box with feeder input	Process scenario*	Feeder box	Test box			Test box with feeder input	Process scenario*
S(A) ($kg\,h^{-1}$)	Rain ($mm\,h^{-1}$)	S(B) ($kg\,h^{-1}$)	S(A) + S(B) ($kg\,h^{-1}$)	S(C) ($kg\,h^{-1}$)		S(A) ($kg\,h^{-1}$)	Rain ($mm\,h^{-1}$)	S(B) ($kg\,h^{-1}$)	S(A) + S(B) ($kg\,h^{-1}$)	S(C) ($kg\,h^{-1}$)	
Treatment 1, Feeder box: rain 100 mm^{-1}; Test box: slope: 5%, +20 cm seepage											
10·8	25	23·5	34·3	50·1	5	15·4	25	18·6	34·0	34·4	4
10·4	50	51·7	62·1	80·5	5	16·4	50	34·2	50·6	56·0	5
10·3	75	86·8	97·1	117·7	5	14·3	75	56·8	71·1	80·0	5
9·6	150	170·9	180·5	205·2	5	13·1	150	121·5	134·6	142·3	5
Treatment 2, Feeder box: rain 150 mm^{-1}; Test box: slope: 5%, +20 cm seepage											
17·2	25	9·4	26·6	27·8	4	15·7	25	14·8	30·5	40·7	5
17·0	50	28·2	45·2	54·1	5	16·6	50	33·4	50·0	65·7	5
16·3	75	41·1	57·4	67·9	5	14·5	75	51·0	65·5	90·2	5
15·2	150	99·2	114·4	123·8	5	13·8	150	108·0	121·8	134·9	5
Treatment 3, Feeder box: rain 100 $mm\,h^{-1}$; Test box: slope: 5%, –20 cm drainage											
9·0	25	1·6	10·6	6·1	1	8·2	25	1·4	9·6	5·4	1
9·1	50	4·5	13·6	9·5	2	7·4	50	4·1	11·5	9·3	2
8·5	75	13·5	22·0	21·2	4	7·8	75	12·4	20·2	21·5	4
7·9	150	28·6	36·5	34·4	3	7·6	150	37·1	44·7	43·3	4
Treatment 4, Feeder box: rain 150 $mm\,h^{-1}$; Test box: slope 5%, –20 cm drainage											
19·4	25	2·8	22·2	15·3	1	20·0	25	1·9	21·9	9·6	1
23·2	50	6·6	29·8	21·3	2	23·8	50	5·9	29·7	16·5	1
17·2	75	19·9	37·1	41·1	5	17·1	75	13·7	30·8	29·1	4
16·2	150	52·0	68·2	67·7	4	15·9	150	44·3	60·2	60·5	4
Treatment 5, Feeder box: rain 150 $mm\,h^{-1}$; Test box: slope: 10%, –10 cm drainage											
10·5	25	3·6	14·1	14·7	4	10·0	25	4·5	14·5	17·5	5
11·4	50	9·9	21·3	23·5	5	10·3	50	11·9	22·2	27·2	5
9·3	75	22·0	31·3	37·2	5	8·9	75	26·7	35·6	41·3	5
12·4	150	74·3	86·8	89·4	5	8·4	150	69·9	78·3	94·4	5
Treatment 6, Feeder box: rain 150 $mm\,h^{-1}$; Test box: slope: 10%, –10 cm drainage											
17·9	25	4·1	22·0	23·4	4	19·8	25	5·7	25·5	32·0	5
20·6	50	10·8	31·4	33·5	5	20·6	50	16·7	37·3	47·9	5
15·7	75	23·0	38·7	46·3	5	17·6	75	28·8	46·4	56·9	5
25·9	150	73·8	99·7	111·4	5	16·4	150	78·9	95·3	115·2	5

* Scenario 1, S(C) < S(A); 2, S(C) = S(A); 3, S(A) < (S(C) < (S(A) + S(B)); 4, S(C) = (S(C) = (S(A) + S(B)); 5, S(C) > (S(A) + S(B))

Figure 2. Soil surface morphology after a run made under drainage conditions showing crescent-shaped surface scours

Figure 3. Soil surface morphology after a run made under seepage conditions showing severe rilling

similar to those under seepage conditions. Making runs first under seepage and later under drainage conditions from the same soil box further ensured a similar surface morphology between seepage and drainage runs, and changes in sediment delivery were indeed only caused by the reversal of the near-surface hydraulic gradient. Data in Table II showed that under both rainfall intensities, i.e. 50 and 100 mm h^{-1}, sediment delivery was greatly reduced either with or without the feeder input as the soil box was shifted from a seepage condition to a drainage one. The data also indicate an interaction between upslope (feeder) sediment content and sediment detachment in the downslope test box. (A detailed discussion on the upslope sediment effects is presented by Zheng *et al.* (1998).) This data set provides

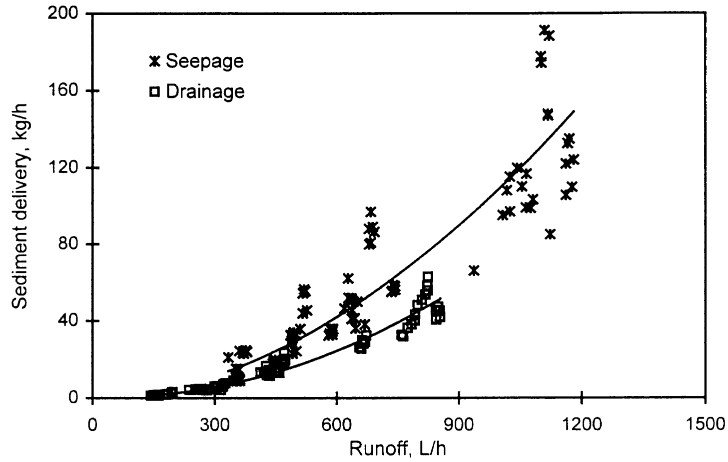

Figure 4. Sediment delivery from the test box without feeder under seepage and drainage conditions

additional confirmation to the attribution of seepage condition as a key factor for increased rilling and erosion on hillslopes. (Huang and Laflen, 1996; Gabbard *et al.*, 1998).

Erosion process scenario

Runoff data shown in Table III indicated a reasonable water balance between total runoff from both boxes separated, i.e. $R(\mathrm{A}) + R(\mathrm{B})$, and the runoff from the test box with feeder input $R(\mathrm{C})$. On the other hand, erosion process scenarios shown in Table IV depicted all five possible scenarios but appeared to follow distinct patterns as both surface hydrologic condition and slope gradient were changed. Therefore, the existence of different sediment scenarios cannot be attributed to runoff intensity alone and has resulted from changes in surface condition and slope gradient.

Under drainage conditions at 5 per cent slope, the erosion process in the test box changed from net deposition (Scenario 1) to equilibrium (Scenario 4) as the rainfall intensity was increased from 25 to 150 mm h^{-1}. The occurrence of a Scenario 5 situation at 75 mm h^{-1} rainfall intensity may have been caused by the variability in surface condition and sampling error. When the slope steepness was increased to 10 per cent or when the hydrologic condition was changed to seepage conditions, the erosion process mostly followed Scenario 5, i.e. the feeder water caused additional sediment delivery from the test box, except that some Scenario 4 cases occurred under 25 mm h^{-1} rainfall.

The Scenario 1 net deposition in the test box is caused by both excessive sediment input from the feeder box and insufficient sediment-carrying capacity of the flow in the test box at low slope and rainfall intensity. This scenario is possible because the feeder box was set to 10 per cent slope and rained at either 100 or 150 mm h^{-1} while the test box was at 5 per cent slope and under 25 to 50 mm h^{-1} rainfall. In field conditions, Scenario 1 simulates erosion processes at a concave shoulder portion of a hillslope or runoff from a highly erosive and erodible region to a lower one. An increase in raindrop impact and flow transport from increased rainfall intensity shifted the sediment deposition regime to an equilibrium condition at which the runon water and sediment from the feeder box caused neither additional detachment nor deposition in the test box.

Under seepage conditions, the soil strength is low and sediment is easily detached and transported. The flow from the runon water caused additional sediment delivery from the test box. The change in slope gradient to 10 per cent increased the sediment transport capacity of the flow, despite an increased

soil strength under drainage conditions; the increased sediment transport capacity also brought forth additional sediments from the test box. The process of additional flow detachment for the Scenario 5 situation is therefore triggered by increasing either soil erodibility or flow transport capacity. Scenario 5 can be considered as a transport-dominated regime in the sense that sediment delivery is dictated by the flow transport capacity because of low soil strength and high flow shear. In field conditions, the Scenario 5 regime represents processes at the backslope or footslope locations.

Sediment transport capacity: contradictions and reality

Data from the dual-box study presented in Table IV revealed contradictions and challenges to the sediment transport capacity concept in the current US erosion process model, i.e. WEPP derived form the Foster–Meyer model. In this model, the transport capacity, T_c, sets the upper limit of sediment transport and a *transport-limiting* (TL) sediment regime indicates that sediment in the runoff has reached its maximum capacity. Under the TL regime, any additional sediment added to the runoff would be deposited. The association of the deposition process with the TL regime is the basis of several experimental studies designed to quantify T_c (Lu *et al*., 1989; Lu and Khan, 1992). Our data from the 5 per cent slope, drainage conditions and 25 mm h^{-1} rainfall appeared to be an example of the TL deposition process. The sediment discharge rates of 5 to 15 kg h^{-1} obtained under 5 per cent slope and 25 mm h^{-1} rainfall with both low and high feeder inputs could be considered as the values of T_c for runoff intensities ranging from 330 to 480 l h^{-1}.

Recent papers on surface hydrologic conditions and sediment regimes have associated a TL regime to seepage conditions and a *detachment-limiting* (DL) sediment regime to drainage conditions because the increased soil strength would limit the amount of sediment detachment and, consequently, transport (Gabbard *et al*., 1998; Huang, 1998). Therefore, it is likely that the soil box at 5 per cent slope and drainage conditions is also in a DL regime. This drainage-associated DL regime is further supported by the sediment data from seepage conditions. Under seepage conditions, rainfall at 25 mm h^{-1} alone without added inflow produced sediment rates ranging from 9 to 24 kg h^{-1} with runoff intensities from 355 to 447 l h^{-1}. Apparently, the flow under seepage conditions can carry more sediment than the flow under drainage conditions for identical rainfall and similar runoff intensities. If the sediment under the seepage condition is under a TL regime, then the lower sediment rates from the drainage condition would imply a DL sediment regime. The apparent coexistence of TL and DL regimes for the drainage condition is a contradiction.

Another data set that showed the apparent TL and DL contradiction is from 5 per cent slope, 50 mm h^{-1} rainfall with a high sediment addition. A Scenario 1 deposition regime was assigned to the drainage condition with total sediment delivery ranging from 17 to 21 kg h^{-1} and runoff intensities from 597 to 608 l h^{-1}. Alone without the feeder input, the sediment delivery at 50 mm h^{-1} rainfall under seepage conditions ranged from 28 to 51 kg h^{-1} while the runoff varied from 492 to 577 l h^{-1}. Lesser runoff under seepage conditions produced a greater amount of sediment as compared to a slightly greater runoff under drainage conditions with an apparent deposition but a lower amount of sediment delivery: again, a TL–DL contradiction.

Another way of phrasing the TL–DL contradiction is: 'If sediment delivery is already at its T_c under drainage conditions, from the evidence of deposition, then what would be the meaning of greater sediment delivery rates under seepage conditions without signs of deposition?' These contradictions indicate that there is a need to revise the current transport capacity concept and its relationships to detachment and deposition in developing process-based erosion models.

Revised sediment transport and erosion process model concept

Our data suggested that sediment transport capacity is not just a function of sediment properties and flow hydraulics, as currently known and used in 'process-based erosion models'. Surface hydrologic

conditions, such as seepage and drainage, affect soil erodibility and have an important role in controlling the transport capacity and sediment regime. Many alternatives are possible in reformulating the erosion process model concept.

One alternative is to redefine sediment transport capacity as a function of soil properties, flow hydraulics and surface conditions and still use a detachment–transport coupling model such as the Foster–Meyer model to relate T_c and q_s to sediment detachment and deposition. If the erosion process model continues to use T_c as the criterion for erosion process separation, the value of T_c has to be quantified for many different surface conditions as demonstrated in this study. One problem still remaining is how to measure T_c experimentally. The dual-box system is excellent in studying erosion processes, but not suitable for routine soil testing because of the large quantity of soil needed to fill the box and the extensive preparation work required for each run. Since seepage cannot be readily recreated in the field, the experimental procedure probably has to be conducted in the laboratory. It is a challenge for erosion scientists to come up with a procedure for measuring T_c.

Another alternative is to use the Meyer–Wischmeier concept with separate detachment and transport components for DL and TL sediment regimes. From a field study on three midwestern soils, Huang *et al.* (1996) showed the advantage of using the Meyer–Wischmeier model to describe sediment detachment and transport in flow channels. Recent laboratory rainfall simulation studies also showed distinctive DL and TL regimes associated with drainage and seepage conditions (Gabbard *et al.,* 1998; Huang, 1998). Although the Meyer–Wischmeier model concept may appear to be a better alternative than the Foster–Meyer model, the difficulty is to identify the proper sediment regime and functional relationships for a specific regime under different rainfall, slope and soil surface conditions. Still, the association of the deposition process with a TL regime in the Meyer–Wischmeier model is an area that needs to be revised.

Instead of fitting a preconceived DL/TL process regime, the most logical approach seems to be the Rose model concept. The Rose model is a dynamic model with separate but simultaneous detachment, transport and deposition components. The dynamic balance dictates the controlling erosion process and sediment regime. In fact, changes from Scenario 1 to 5 may be caused by the shift in the dynamic balance from a deposition-dominated (Scenario 1) to detachment-dominated (Scenario 3) and finally a transport-dominated (Scenario 5) process regime. Scenario 2 is a transition between deposition- and detachment-dominated processes, and likewise, Scenario 4 is a transition between detachment and transport. The transition from Scenario 2 to Scenario 4 regimes may be explained by the re-entrainment concept, a further development of the Rose model to account for the redetachment of already detached and subsequently deposited sediment (Hairsine and Rose, 1992). To test the re-entrainment concept, experimental procedures need to be developed to partition the total sediment delivery to its source areas. Until such procedures are in place, the re-entrainment concept will remain a hypothetical one.

The advantage of using a dynamic equilibrium model with simultaneous detachment, transport and deposition processes alleviates the potential contradiction in the detachment/transport-limiting model concept. The designation of a particular sediment process scenario, as the outcome of the sediment mass balance, is to identify the dominating process occurring on the hillslope. Our data have shown a general trend for increasing slope steepness, rainfall intensity and soil erodibility to cause the shift in erosion process regime from Scenario 1 to 5. If the sediment delivery from the 5 m test box represents a dynamic equilibrium for the specific condition, i.e. slope gradient, hydrologic condition, and rainfall and runoff intensities, these data can then be used to quantify the association between surface condition and the erosion processes. This hypothesis is currently being tested in the laboratory and preliminary results are promising.

CONCLUSIONS AND IMPLICATIONS

Results of this study demonstrated the capability of a dual-box system to quantify erosion process scenarios from deposition-dominated to transport-dominated regimes. Our data show: (1) sediment regime from the dual-box system can be categorized into five different sediment scenarios ranging from

deposition-dominated to detachment- and transport-dominated processes; (2) the dominant erosion process depends on slope gradient, rainfall intensity and soil erodibility; and (3) an increase in soil erodibility from the seepage condition triggers a transport-dominated regime while a decrease in soil erodibility from profile drainage limits sediment detachment and enhances sediment deposition. These scenarios were used to compare three proposed erosion process model concepts: Meyer–Wischmeier, Foster–Meyer and Rose models. The Rose model, which contains simultaneous deposition, detachment and transport processes, appears to best describe the experimental findings. These findings may change future directions of erosion process research and prediction model development.

Erosion process model concepts have been proposed for many years, dating back to the pioneering works of Ellison (1944, 1947a, b, c), and are currently used in the development of process-based erosion prediction models. Physical processes of deposition, detachment and transport are well recognized in the conceptual development of erosion models. Unfortunately, experimental procedures to test conditions when all these processes are occurring have not been developed until recently. This dual-box system allows us to examine conditions for different process scenarios.

Besides testing for different sediment scenarios, the dual-box system is capable of simulating those processes occurring at a portion of a hillslope. Changes in slope gradient, rainfall distribution and soil erodibility, and their effects on erosion processes, can be quantified by setting different conditions for the feeder and test boxes. Experiments have begun to evaluate the upslope runon sediment effects on erosion processes downslope, by changing the sediment-to-water ratio of the feeder input. An expansion of the dual-box system to a triple-box setup is near completion and experiments will begin soon to quantify sediment transport processes in a complex slope geometry. These recent developments in laboratory soil-box procedures will yield valuable information for the understanding of erosion processes occurring at a scale similar to that occurring on hillslopes.

ACKNOWLEDGEMENT

The authors would like to thank Professor Fenli Zheng, Institute of Soil and Water Conservation, Yangling, Shaanxi, China, for providing the data set tabulated in Table II showing seepage and drainage effects from her study on run-on water and sediment effects.

REFERENCES

Ellison, W. D. 1944. 'Studies of raindrop erosion', *Agricultural Engineering*, **25**, 131–136, 181–182.

Ellison, W. D. 1947a. 'Soil erosion studies – Part I', *Agricultural Engineering*, **28**, 145–146.

Ellison, W. D. 1947b. 'Soil erosion studies – Part II: Soil detachment hazard by raindrop splash', *Agricultural Engineering*, **28**, 197–201.

Ellison, W. D. 1947c. 'Soil erosion studies – Part V: Soil transportation in the splash process', *Agricultural Engineering*, **28**, 349–353.

Ellison, W. D. and Ellison, O. T. 1947a. 'Soil erosion studies – Part VI: Soil detachment by surface flow', *Agricultural Engineering*, **28**, 402–408.

Ellison, W. D. and Ellison, O. T. 1947b. 'Soil erosion studies – Part VII: Soil transportation by surface flow', *Agricultural Engineering*, **28**, 442–444, 450.

Foster, G. R. and Meyer, L. D. 1972. 'A closed-form soil erosion equation for upland areas', in Shen, H. W. (Ed.), *Sedimentation*. Colorado State University, Ft Collins, Colorado, 12-1–12-19.

Foster, G. R. and Meyer, L. D. 1975. 'Mathematical simulation of upland erosion by fundamental erosion mechanics', in *Present and prospective technology for predicting sediment yields and sources*, US Department of Agriculture, Agricultural Research Service, Southern Region, New Orleans, Louisiana, **ARS-S-40**, 190–207.

Foster, G. R., Eppert, F. P. and Meyer, L. D. 1979. 'A programmable rainfall simulator for field Plots', *Proceedings of Rainfall Simulator Workshop*, 7–9 March 1979, Tucson, Arizona, US Department of Agriculture, Science and Education Administration, Agricultural Reviews and Manuals, ARM-W-10, 45–59.

Gabbard, D. S., Huang, C., Norton, L. D. and Steinhardt, G. C. 1998. 'Landscape position, surface hydraulic gradients and erosion processes', *Earth Surface Processes and Landforms*, **23**, 83–93.

Hairsine, P. B. and Rose, C. W. 1992. 'Modeling water erosion due to overland flow using physical principles: 1. Sheet flow', *Water Resources Research*, **28**, 237–243.

Huang, C. 1998. 'Sediment regimes under different slope and hydrologic conditions', *Soil Science Society of America Journal*, **62**, 423–430.

Huang, C. and Laflen, J. M. 1996. 'Seepage and soil erosion for a clay loam soil', *Soil Science Society of America Journal*, **60**, 408–416.

Huang, C., Bradford, J. M. and Laflen, J. M. 1996. 'Evaluation of the detachment–transport coupling concept in the WEPP rill erosion equation', *Soil Science Society of America Journal*, **60**, 734–739.

Lu, J. Y. and Khan, M. J. 1992. 'Uniqueness of transport capacity of uniform and graded sediment under rainfall', In Larsen, P. and Eisenhauer, N. (Eds), *Sediment Management: Proceedings of 5th International Symposium on River Sedimentation*, Karlsruhe, Germany, 443–450.

Lu, J. Y., Cassol, E. A. and Moldenhauer, W. C. 1989. 'Sediment transport relationships for sand and silt loam soils', *Transactions of American Society of Agricultural Engineers*, **36**, 1923–1931.

Meyer, L. D. and Wischmeier, W. H. 1969. 'Mathematical simulation of the process of soil erosion by water', *Transactions of American Society of Agricultural Engineers*, **12**, 754–758, 762.

Meyer, L. D., Foster, G. R. and Romkens, M. J. M. 1975. 'Source of soil eroded by water from upland slopes', in *Present and prospective technology for predicting sediment yields and sources*, US Department of Agriculture, Agricultural Research Service, Southern Region, New Orleans, Louisiana, **ARS-S-40**, 177–189.

Nearing, M. A., Foster, G. R., Lane, L. J. and Finkner, S.C. 1989. 'A process-based soil erosion model for USDA-Water Erosion Prediction Project technology', *Transactions of American Society of Agricultural Engineers*, **32**, 1587–1593.

Rose, C.W. 1985. 'Developments in soil erosion and deposition models', *Advances in Soil Science*, **2**, 1–63.

Rose, C. W., Williams, J. R., Sander, G. C. and Barry, D. A. 1983. 'A mathematical model of soil erosion and deposition processes: I. Theory for a plane land element', *Soil Science Society of America Journal*, **47**, 991–995.

Zheng, F., Huang, C. and Norton, L.D. 1998. 'Run-on water and sediment effects on erosion processes and sediment regimes', *Soil Science Society of America Journal*, (submitted).

